

Influence of dipolar interactions on hyperthermia properties of ferromagnetic particles

D. Serantes, D. Baldomir, C. Martinez-Boubeta, K. Simeonidis, M. Angelakeris et al.

Citation: *J. Appl. Phys.* **108**, 073918 (2010); doi: 10.1063/1.3488881

View online: <http://dx.doi.org/10.1063/1.3488881>

View Table of Contents: <http://jap.aip.org/resource/1/JAPIAU/v108/i7>

Published by the [American Institute of Physics](http://www.aip.org).

Related Articles

Fe₃O₄-citrate-curcumin: Promising conjugates for superoxide scavenging, tumor suppression and cancer hyperthermia

J. Appl. Phys. **111**, 064702 (2012)

Integrated intravital microscopy and mathematical modeling to optimize nanotherapeutics delivery to tumors

AIP Advances **2**, 011208 (2012)

In vitro cytotoxicity of Selol-loaded magnetic nanocapsules against neoplastic cell lines under AC magnetic field activation

J. Appl. Phys. **111**, 07B335 (2012)

Magnetically driven spinning nanowires as effective materials for eradicating living cells

J. Appl. Phys. **111**, 07B329 (2012)

Experimental characterization of electrochemical synthesized Fe nanowires for biomedical applications

J. Appl. Phys. **111**, 056103 (2012)

Additional information on *J. Appl. Phys.*

Journal Homepage: <http://jap.aip.org/>

Journal Information: http://jap.aip.org/about/about_the_journal

Top downloads: http://jap.aip.org/features/most_downloaded

Information for Authors: <http://jap.aip.org/authors>

ADVERTISEMENT



**FIND THE NEEDLE IN THE
HIRING HAYSTACK**

Post jobs and reach
thousands of hard-to-find
scientists with specific skills



<http://careers.physicstoday.org/post.cfm> **physicstoday** JOBS

Influence of dipolar interactions on hyperthermia properties of ferromagnetic particles

D. Serantes,¹ D. Baldomir,^{1,a)} C. Martínez-Boubeta,^{2,a)} K. Simeonidis,³ M. Angelakeris,³ E. Natividad,⁴ M. Castro,⁴ A. Mediano,⁵ D.-X. Chen,⁶ A. Sanchez,⁶ Ll. Balcells,⁷ and B. Martínez⁷

¹Departamento de Física Aplicada, Instituto de Investigaciones Tecnológicas, Universidad de Santiago de Compostela, 15782 Santiago de Compostela, Spain

²IN2UB and Departament d'Electrònica, Universitat de Barcelona, Martí i Franquès 1, 08028 Barcelona, Spain

³Department of Physics, Aristotle University of Thessaloniki, 54124 Thessaloniki, Greece

⁴Instituto de Ciencia de Materiales de Aragón, CSIC-Universidad de Zaragoza, Sede Campus Río Ebro, María de Luna 3, 50018 Zaragoza, Spain

⁵Grupo de Electrónica de Potencia y Microelectrónica (GEPM), Instituto de Investigación en Ingeniería de Aragón, Universidad de Zaragoza, María de Luna 3, 50018 Zaragoza, Spain

⁶Departament de Física, ICREA, Universitat Autònoma de Barcelona, 08193 Bellaterra, Spain

⁷ICMAB-CSIC, Campus UAB, 08193 Bellaterra, Spain

(Received 23 June 2010; accepted 4 August 2010; published online 8 October 2010)

We show both experimental evidences and Monte Carlo modeling of the effects of interparticle dipolar interactions on the hysteresis losses. Results indicate that an increase in the intensity of dipolar interactions produce a decrease in the magnetic susceptibility and hysteresis losses, thus diminishing the hyperthermia output. These findings may have important clinical implications for cancer treatment. © 2010 American Institute of Physics. [doi:10.1063/1.3488881]

I. INTRODUCTION

About half a century ago, the search of a method to pasteurize the nodes which contain cancer metastases missed at surgical interventions, motivated investigations on the magnetic properties of iron oxide nanoparticles (NPs) which would heat appreciably at radio frequencies after injection into lymphatic channels.¹ Since then, *in vitro* experiments with magnetic fluids have confirmed their excellent power absorption capabilities.² *In vivo* experiments have documented the feasibility of this treatment in animal models of melanoma,³ breast tumors,⁴ and prostate cancer.⁵ Depending on the applied temperature and the duration of heating this treatment either results in direct tumor cell killing or makes the cells more susceptible to concomitant radio—or chemotherapy, thus increasing therapeutic efficiency.

The heating power of magnetic NPs is determined by several factors including particle type, the frequency of the radiated alternating magnetic field and the magnetic field intensity. Namely, there are two mechanisms to account for heat generation of magnetic of NPs less than about 30 nm in diameter: (a) Néel relaxation, that is, the fluctuation of a crystal's magnetic moment over an anisotropic energy barrier and (b) Brown relaxation to viscous losses due to particle reorientation in solution.⁶ Given that, for clinical practice,⁷ Brownian contributions to ac losses are eliminated in the case of immobilized particles,⁸ larger particles (showing ferromagnetic hysteresis) seem a better choice for these applications using alternating magnetic fields below the megahertz range.⁶

On the other hand, the losses due to magnetization reori-

entation in ferromagnetic particles depend on the type of remagnetizing process which, besides the intrinsic magnetic properties—like magnetocrystalline anisotropy—is determined in complicated ways by particle size, shape and microstructure. Modeling of the performance of magnetic NPs in hyperthermia has been previously reported.^{9,10} However, it has not been clarified yet if an increase in the concentration of particles leads to an increase in the heating capacity, or to a decrease as recently suggested by Urtizberea *et al.*¹¹ Therefore, the use of Monte Carlo (MC) simulation methods could be of valuable help to analyze the performances of ferromagnetic NPs for hyperthermia applications. Our previous results demonstrated that nanostructured Fe NPs coated with a uniform MgO epitaxial shell may act as high performance therapy vectors with similar heating power of existing materials but at much more lower doses.¹² It was anticipated that a ferromagnetic coupling between NPs might result in a decreased hysteresis and hence in a diminished heating ability. We shall report here the effect of particle concentration on the magnetic hysteresis of the monodisperse NP assemblies by comparing our own experimental data with MC simulations. This study aims in the explanation of the role played by interparticle dipolar interactions and the optimization of the solution properties for hyperthermia applications.

II. EXPERIMENTAL RESULTS

The studied nanostructures consist of spherical zero-valence ferromagnetic Fe particles (~ 75 nm) with a MgO coating for biocompatibility. Figure 1 shows a ferromagnetic behavior well above room temperature (RT). The effective anisotropy constant ($K \approx 4.5 \times 10^4$ J/m³) and saturation magnetization ($M_S = 210$ emu/g) values are very close to

^{a)}Electronic addresses: daniel.baldomir@usc.es and cboubeta@el.uib.es.

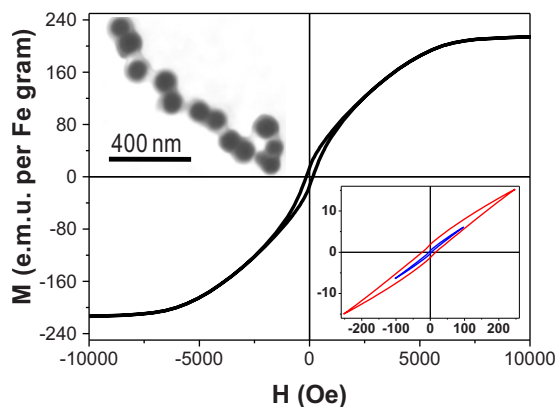


FIG. 1. (Color online) Field dependent magnetization curve at room temperature of the Fe core/MgO shell NPs. Inset on the left shows an electron microscopy image of the NPs arranged in a chain resembling a magnetosome (Ref. 29). The inset on the right exhibits minor hysteresis loops.

that of bulk bcc Fe. A detailed structural, morphological and magnetic characterization of the samples has been already published.^{12,13} At low concentrations, particles are prone to appear in the form of interconnected chainlike structures, thus demonstrating strong dipolar interactions.¹⁴

In order to assess the effects of dipolar interactions on the NP intrinsic magnetic properties, particles were diluted at different concentrations into distilled water or ethanol. Magnetic hyperthermia experiments were carried out under various ac magnetic fields by means of a water cooled induction coil of 23 mm diameter consisting of three turns, and a commercial generator with a power of 4.5 kW.¹² The heating efficiency is quantified by the specific absorption rate (SAR), actually by measuring the initial slope of the temperature rise before the effect of heat conduction becomes important.¹⁵ Adiabatic SAR measurements were performed on particles dispersed in an epoxy matrix by a calorimetric method described in Ref. 16. Such experiments allowed quantifying accurately the small heating powers generated at low concentration and low ac fields. It is widely believed that the heating effect is a result of energy absorption from the alternating magnetic field and its transformation into heat by means of the hysteresis loss during reversal of magnetization. For that reason, and for the sake of comparison, the loss power was also determined from hysteresis losses in powder samples measured by using a superconducting quantum interference device magnetometer, by taking into account the proportionality of power with frequency.¹⁷ Please note that in magnetic hyperthermia applications, the frequencies of the alternating magnetic fields are several orders of magnitude higher than those frequencies applied by the magnetometer to measure the energy dissipation per cycle.

Alternative methods for quantifying SAR were also applied. Still, the ac susceptibility $\chi = \chi' - j\chi''$ of magnetic liquids was measured as a function of ac field amplitude and frequency, by using a home-made high-field ac susceptometer.¹⁸ Although a linear frequency dependence is usually assumed, in real magnetic liquids one may observe deviations from the ideal Debye-like behavior. In our case, the imaginary part of the susceptibility exhibits a maximum below 10 mT, where particle interactions cause a slight fre-

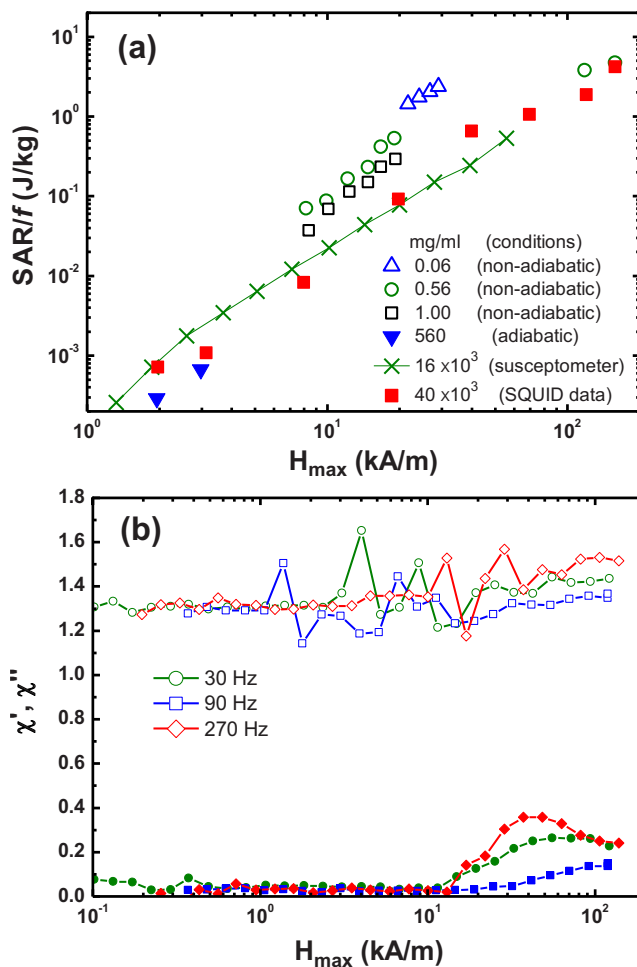


FIG. 2. (Color online) (a) Magnetic hysteresis losses (SAR) in dependence on the magnetic field amplitude for different experimental conditions and concentrations. Adiabatic conditions refer to experiments performed following Ref. 16; nonadiabatic conditions refer to conventional hyperthermia measurements in ferrofluids at different concentrations, and susceptometer refers to experiments performed following Ref. 18. (b) Susceptibility measured at RT as functions of ac field amplitude (H_{\max}) and frequency.

quency dependence in the position of the maximum. These effects, illustrated in Fig. 2, are in agreement with the conclusion drawn by Morozov *et al.*¹⁹ on the frequency dependence of the susceptibility of colloid suspensions with different particle concentrations. Such deviations have usually been attributed to interparticle interactions.²⁰

In other words, susceptibility measurements indicate an interaction exists,²¹ and this interaction increases with particle volume fraction. In addition, the very low relative remanence ($M_R < 0.2$) in Fig. 1, compared to an assembly of noninteracting randomly oriented particles ($M_R = 0.5$),²² explains the reduction in SAR values on increasing the particles' concentration [Fig. 2(a)]. It appears that increasing concentration reduces the magnetic hysteresis due to dipolar coupling effects, as has also been suggested in previous works reporting similar SAR versus magnetic field evolution.^{11,23} However, the cause of such decrease remains still unclear, being also conjectured to originate from a broad size distribution. Thus, with the purpose of studying the role of magnetic dipolar interactions on the hyperthermia proper-

ties of the NP system, we performed MC simulations to treat the influence of particle concentration and field dependence on the SAR.

III. MODELIZATION AND DISCUSSION

The physical model employed for our numerical simulations considers the usual approximation of single-domain magnetic NPs with an effective uniaxial magnetic anisotropy \vec{K}_{eff} which may be of magnetocrystalline or shape origin. We also assume that every i -particle has uniform magnetization and composition, and all its atomic moments rotate coherently, so that the magnetic moment of each particle is $|\vec{\mu}| = M_S V$ and $\vec{K}_{eff} = KV\hat{n}$, with \hat{n} the unit vector along the easy-axis direction and V the particle's volume. The spatial distribution of the particles resembles a frozen ferrofluid without aggregations, the positions of the particles are kept fixed and the easy axes are chosen randomly. Aiming to focus on the role of the dipolar interparticle interactions we have simplified the system in order to set very ideal conditions, assuming (i) temperature-independent K , V , and M_S and (ii) a perfectly monodisperse system. The energy model is the same as in Ref. 24 so that the energy of each particle in this ideal scenario is regarded to have three main sources: anisotropy (E_A), Zeeman (E_H) and dipolar interaction (E_D). The uniaxial-type anisotropy of each i -particle is given by $E_A^{(i)} = -KV(\vec{\mu}_i \cdot \hat{n}_i / |\vec{\mu}_i|)^2$, the influence of the external magnetic field \vec{H} is treated in the usual way $E_Z^{(i)} = -\vec{\mu}_i \cdot \vec{H}$, and the magnetic dipolar interaction energy among two particles i, j located at positions \vec{r}_i, \vec{r}_j is given by $E_D^{(i,j)} = \vec{\mu}_i \cdot \vec{\mu}_j / r_{ij}^3 - 3(\vec{\mu}_i \cdot \vec{r}_{ij})(\vec{\mu}_j \cdot \vec{r}_{ij}) / r_{ij}^5$, with r_{ij} the distance between both particles. The total energy of the system is therefore the summation of these energies extended to all particles.

In our simulations, we reproduce $M(H)$ curves at different sample concentrations (c) and for different values of maximum applied field H_{max} , using the parameter values extracted from the MgO-coated Fe NPs as described above. The process to simulate a $M(H)$ curve starts by first thermalizing the system at zero field from a very high temperature to the desired chosen temperature. Next, the magnetic field is applied and increased in small intervals until a certain H_{max} value; then it is decreased down to $-H_{max}$, and increased again up to H_{max} so that the cycle is complete. To simulate the time-dependence of the magnetization between two field conditions we use the Metropolis algorithm with local dynamics,²⁴ i.e., the particles are allowed to change their configuration a certain amount of trials. In each step, a new orientation of the magnetic moment is generated inside a cone of radius $\delta\theta$ around the actual orientation.²⁵ The energy variation ΔE is calculated and the change to the new orientation is then accepted with probability $\min[1, \exp(-\Delta E/k_B T)]$, with k_B the Boltzmann constant. For a system of N -particles, the repetition of this process N times by randomly picking the particles defines one MC step. The magnetization of the system is recorded after a certain amount of MC steps as the projection of the magnetic moments along the field direction.

With the purpose of illustrating the overall working of the program, Fig. 3(a) shows the $M(H)$ curve for the very

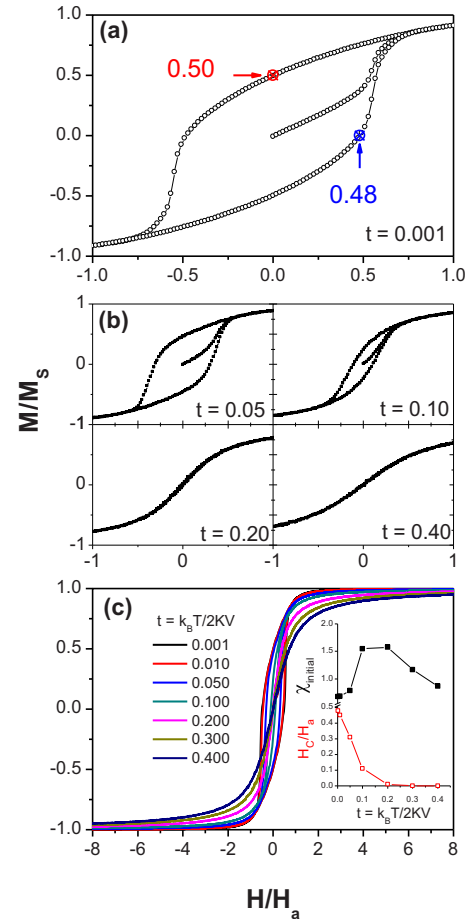


FIG. 3. (Color online) (a) Magnetization vs magnetic field curve in the ideal diluted limit at low temperatures, used as control for setting the amount of MC steps reproducing the Stoner–Wohlfarth conditions, as indicated by the arrows. (b) $M(H)$ curves at increasing temperatures (reduced units $t = k_B T / 2KV$) that illustrate the decrease in hysteresis and H_C with temperature. (c) $M(H)$ curves at different temperatures showing the common saturation behavior at very high fields. Inset shows the temperature dependence of the initial dM/dT susceptibility (upper curve, full squares), and of the coercive field H_C/H_a (lower curve, empty squares).

diluted sample $c=0.0001$ (0.01% volume fraction). We have considered a system of $N=1000$ particles and magnetization results are obtained from averaging the magnetization of all the particles in the system over five different configurations, and for all simulations the field variation ratio was kept constant as $\Delta H=10$ Oe every 400 MC steps. This ratio was chosen so that both the remanence and the coercive field (H_C) in the ideal noninteracting case at very low temperatures reproduce the expected values $M_R \approx 0.50$ and $H_C \approx 0.48 H_a$,¹⁹ where $H_a=2 K/M_S$ is the anisotropy field of the particles. Since the H_a -value is of primary importance in determining the magnetic properties of particle systems, because it weights the relative importance of the Zeeman energy,²⁶ in our simulations we emphasize the value of the external field in relation with H_a .

Some $M(H)$ curves at higher temperatures (treated by means of usual computational reduced temperature units $t = k_B T / 2KV$) (Ref. 24) are plotted in Fig. 3(b) showing the reduction in the hysteresis area with larger temperatures, as expected: the higher thermal energy promotes larger fluctuations in the orientation of the magnetic moments, until at

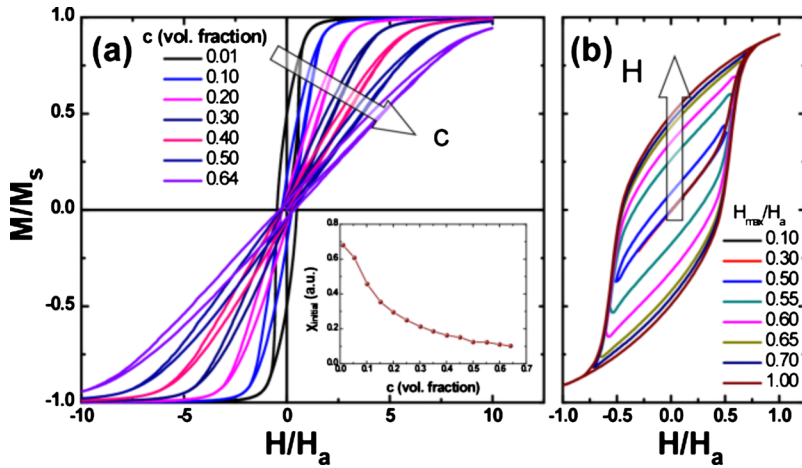


FIG. 4. (Color online) (a) Field dependent magnetization curves for increasing sample concentration; inset shows the initial susceptibility. (b) Magnetization curves as a function of the magnetic field amplitude for a selected sample concentration ($c=0.007$). In both cases arrow indicates magnitude increasing direction.

high enough temperatures the anisotropy energy wells of the particles are completely overcome and the particles reach the *superparamagnetic* (SPM) state. This process is analyzed in more detail on the inset of Fig. 3(c), where it is plotted the temperature dependence of the initial susceptibility [upper curve, full square symbols] and coercive field [lower curve, empty square symbols]. The initial susceptibility first grows until a maximum is reached, and decays afterwards. This behavior agrees with the tendency observed in *zero field cooling* processes,²⁴ as could be expected since the process starts after thermalization of the magnetic moment in zero field. In fact, paramagnetic-like decay of the initial susceptibility seems to be indicated in the high-temperature regime, as corresponds to the SPM behavior. This reasoning is also supported by the trend followed by the coercive field as a function of the temperature, decreasing H_C with growing temperature until it disappears when reaching the SPM-state temperature range. The data shown in the main panel of Fig. 3(c) illustrates the occurrence of saturation of the $M(H)$ curves at the different temperatures for large fields well above the anisotropy field of the particles.

In Fig. 4(a) simulated $M(H)$ curves are shown as a function of the sample concentration. A decrease in the initial susceptibility with increasing c is observed, so that the stronger the interaction between particles, the lower the hyperthermia response. Our results partially agree with those published by Wang *et al.*²⁷ but run contrary to the findings in polydisperse ferrofluids reported by Jeun *et al.*,²⁸ although we think that the different system analyzed in the latter (sample concentration is described as related to the size distribution, whereas in our case a monodisperse system is assumed) may be responsible for such discrepancy. Figure 4(b) shows magnetization curves as a function of the amplitude of the magnetic field for $c=0.007$, where the importance of the field with respect to H_a is underlined: for fields $H < H_c = 0.48 H_a$ there is almost no noticeable effect in the area of the cycle, whereas for values $H_c < H < H_a$ large increases are observed. No noticeable variations are found for $H > H_a$.

IV. CONCLUSIONS

Modeling of the hysteresis losses of a magnetic fluid with alternating magnetic field reveals that heating is dependent on the particle concentrations. This dependence is ana-

lyzed in detail in Fig. 5. The results show a well defined linear dependence on the field amplitude for the concentrated samples ($c=0.07, 0.15$), and a more complex behavior for the more diluted one ($c=0.007$). As expected, the model predicts that SAR saturates to a constant value for large fields, and despite its simplicity, gives a good quantitative account of the measured data shown in Fig. 2 and also reported in other works (see, for instance, Fig. 3 in Ref. 23), the saturation taking place at larger values for larger concentrations. Our results also emphasize the importance of taking into account the characteristic H_a -field of the particles to set our hyperthermia experimental conditions: it seems that H_a (larger the higher the concentration) gives an estimation of the upper limit for the field amplitude for larger SAR.

In summary, MC simulations of an assembly of monodisperse single domain magnetic particles—liquid like arranged—in thermal equilibrium have shown that interparticle interactions modify the energy barrier, changing the global magnetic behavior of the particle systems. We observe that dipolar interactions between NPs significantly affect the magnetic susceptibility and hysteresis losses, thus implying a considerable reduction in specific heating power for hyperthermia applications.

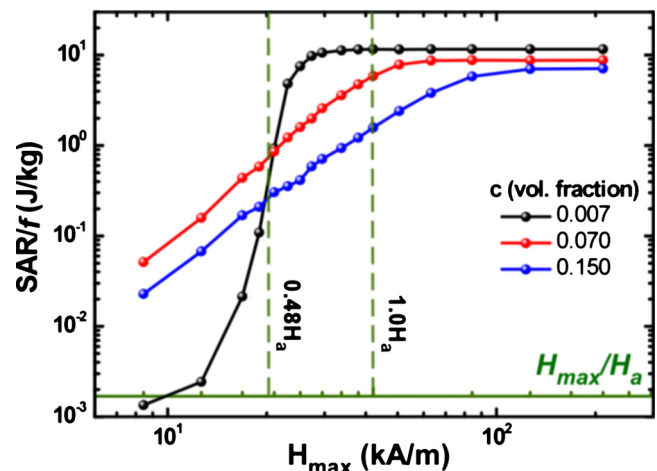


FIG. 5. (Color online) Field-dependence of the SAR for different concentrations ($c=0.007, 0.070, 0.150$). Field data is also expressed in real units in order to make easier the comparison with the experimental values plotted in Fig. 2.

ACKNOWLEDGMENTS

This work was supported by the Greek Secretariat of Research and Technology—Contract No. 03EΔ667 and the Spanish MICINN and FEDER (Project Nos. MAT2009-08024, MAT2009-08165, MAT2007-61621, and CONSOLIDER CSD2007-00041). Xunta de Galicia is acknowledged for project INCITE under Project No. 08PXIB236052PR and for the financial support of D. Serantes (María Barbeito program). C. Boubeta credits support through the Ramón y Cajal program.

- ¹R. K. Gilchrist, R. Medal, W. D. Shorey, R. C. Hanselman, J. C. Parrott, and C. B. Taylor, *Ann. Surg.* **146**, 596 (1957).
- ²A. Jordan, R. Scholz, P. Wust, H. Föhling, and R. Felix, *J. Magn. Magn. Mater.* **201**, 413 (1999); J.-P. Fortin, F. Gazeau, and C. Wilhelm, *Eur. Biophys. J.* **37**, 223 (2008).
- ³A. Ito, K. Tanaka, M. Kondo, M. Shinkai, H. Honda, K. Matsumoto, T. Saida, and T. Kobayashi, *Cancer Sci.* **94**, 308 (2003).
- ⁴I. Hilger, R. Hiergeist, R. Hergt, K. Winnefeld, H. Schubert, and W. A. Kaiser, *Invest. Radiol.* **37**, 580 (2002).
- ⁵M. Johannsen, U. Gneveckow, L. Eckelt, A. Feussner, N. Waldöfner, R. Scholz, S. Deger, P. Wust, S. A. Loening, and A. Jordan, *Int. J. Hyperthermia* **21**, 637 (2005).
- ⁶S. E. Barry, *Int. J. Hyperthermia* **24**, 451 (2008).
- ⁷F. K. H. van Landeghem, K. Maier-Hauff, A. Jordan, K.-T. Hoffmann, U. Gneveckow, R. Scholz, B. Thiesen, W. Brück, and A. von Deimling, *Bio-materials* **30**, 52 (2009).
- ⁸R. Hergt, R. Hiergeist, M. Zeiberger, G. Glöckl, W. Weitscheis, L. P. Ramirez, I. Hilger, and W. A. Kaiser, *J. Magn. Magn. Mater.* **280**, 358 (2004).
- ⁹R. E. Rosensweig, *J. Magn. Magn. Mater.* **252**, 370 (2002).
- ¹⁰S. Purushotham and R. V. Ramanujan, *J. Appl. Phys.* **107**, 114701 (2010).
- ¹¹A. Urtizbera, E. Natividad, A. Arizaga, M. Castro, and A. Mediano, *J. Phys. Chem. C* **114**, 4916 (2010).
- ¹²C. Martinez-Boubeta, L. Balcells, R. Cristòfol, C. Sanfeliu, E. Rodríguez, R. Weissleder, S. Lope-Piedrafita, K. Simeonidis, M. Angelakeris, F. Sandiunenge, A. Calleja, L. Casas, C. Monty, and B. Martínez, *Nanomed. Nano. Biol. Med.* **6**, 362 (2010).
- ¹³C. Martinez-Boubeta, L. Balcells, C. Monty, and B. Martínez, *J. Phys.: Condens. Matter* **22**, 026004 (2010).
- ¹⁴K. Butter, P. H. H. Bomans, P. M. Frederik, G. J. Vroege, and A. P. Philipse, *Nature Mater.* **2**, 88 (2003).
- ¹⁵T. Samaras, P. Regli, and N. Kuster, *Phys. Med. Biol.* **45**, 2233 (2000).
- ¹⁶E. Natividad, M. Castro, and M. Mediano, *Appl. Phys. Lett.* **92**, 093116 (2009).
- ¹⁷R. Hergt, W. Andrá, C. G. d'Ambly, I. Hilger, W. A. Kaiser, U. Richter, and H.-G. Schmidt, *IEEE Trans. Magn.* **34**, 3745 (1998).
- ¹⁸D.-X. Chen, *Meas. Sci. Technol.* **15**, 1195 (2004).
- ¹⁹K. I. Morozov, A. F. Pshenichnikov, Y. L. Raikher, and M. I. Shliomis, *J. Magn. Magn. Mater.* **65**, 269 (1987).
- ²⁰L. M. Lacroix, R. Bel Malaki, J. Carrey, S. Lachaize, M. Respaud, G. F. Goya, and B. Chaudret, *J. Appl. Phys.* **105**, 023911 (2009).
- ²¹M. Hanson, *J. Magn. Magn. Mater.* **96**, 105 (1991).
- ²²E. C. Stoner and E. P. Wohlfarth, *Philos. Trans. R. Soc. London, Ser. A* **240**, 599 (1948).
- ²³R. Hergt, S. Dutz, R. Müller, and M. Zeisberger, *J. Phys.: Condens. Matter* **18**, S2919 (2006).
- ²⁴J. García-Otero, M. Porto, J. Rivas, and A. Bunde, *Phys. Rev. Lett.* **84**, 167 (2000).
- ²⁵An improvement included in the present simulations in comparison with those reported in Ref. 24 is that the trial angle $\delta\theta$ is now temperature-dependent, in the way proposed by U. Nowak, R. W. Chantrell, and E. C. Kennedy, *Phys. Rev. Lett.* **84**, 163 (2000); X. Z. Cheng, M. B. A. Jalil, H. K. Lee, and Y. Okabe, *ibid.* **96**, 067208 (2006). The temperature-dependence is given by $\delta\theta=(0.05 \times k_B T / 2 \text{ KV})^{0.5}$ in the usual reduced units, and reproduces the 0.075 value of Ref. 24 approximately at $t=0.11$.
- ²⁶R. H. Victora, *Phys. Rev. Lett.* **63**, 457 (1989).
- ²⁷A. Wang, J. Li, and R. Gao, *Appl. Phys. Lett.* **94**, 212501 (2009).
- ²⁸M. Jeun, S. Bae, A. Tomitaka, Y. Takemura, K. H. Park, S. H. Paek, and K.-W. Chung, *Appl. Phys. Lett.* **95**, 082501 (2009).
- ²⁹D. A. Bazylinski and R. B. Frankel, *Nat. Rev. Microbiol.* **2**, 217 (2004).